
Trajectory image-guided percutaneous renal cryoablation in a porcine model: a pilot study

David A. Rebeck, MD, Robert B. Nadler, MD, Kent T. Perry, MD

Department of Urology, Northwestern University Feinberg School of Medicine, Chicago, Illinois, USA

REBUCK DA, NADLER RB, PERRY KT. Trajectory image-guided percutaneous renal cryoablation in a porcine model: a pilot study. *The Canadian Journal of Urology*. 2012;19(1):6094-6099.

Introduction: To assess the technical feasibility and safety of trajectory image-guided percutaneous renal cryoablation in a porcine model.

Materials and methods: Six pigs (12 kidneys) were utilized. Only the posterior and lateral regions of the kidneys were considered. A bone-anchored dynamic reference frame (DRF) was inserted into the iliac crest and the O-Arm and StealthStation TREON System (OASSTS, Medtronic, CO, USA) was used to acquire 3-dimensional (3D) imaging of the kidneys. A hand-held pointing device was crafted from a cryoablation needle (Galil Medical, MN, USA) and an optical reference frame. The hand-held pointer/cryoablation needle ("cryoprobe") was then optically recognized by the OASSTS. The cryoprobe was then used to navigate its tip into a randomly chosen renal region of interest using

3D trajectory images. Two freeze-thaw cryoablation cycles were then performed. We assessed treatment times and effective radiation doses. We also assessed concordance between projected iceball location on trajectory imaging and cryolesion location on necropsy.

Results: The mean total treatment time was 24.0 minutes. The mean effective radiation dose was 23.7 mSv per kidney treated. The trajectory-guided images used to place the cryoprobe tips into the renal region of interest agreed with the necropsy-determined location of the cryolesion in all cases. Injury to a lumbar muscle and a renal pelvis were observed in two separate cases, respectively.

Conclusions: Trajectory image-guided percutaneous renal cryoablation using OASSTS is technically feasible, appears safe, and is associated with acceptable levels of radiation exposure. Comparison of trajectory image-guidance and cryolesions on necropsy demonstrated concordant needle placement.

Key Words: cryoablation, image-guided, navigation, percutaneous, trajectory

Introduction

Cryoablation is a nephron-sparing approach to the treatment of small renal masses.¹ It has been applied in both the laparoscopic and percutaneous settings. Advantages of the percutaneous approach include decreased pain and blood loss, shorter hospitalization and improved cost-effectiveness.^{2,3} Disadvantages, however, may include a lower primary treatment

success rate.³ Computed-tomography (CT) has been the most widely used form of imaging for the percutaneous approach. Traditional CT-guidance, however, does not provide real-time guided imaging, provides only orthogonal planes to perform needle placement, and treatment session times can be lengthy. The O-Arm and StealthStation TREON System (OASSTS, Medtronic, CO, USA) is a surgical navigation technology that allows for trajectory imaging (which displays anatomy in the plane of the trajectory of a pointing device, while the pointing device itself is displayed as a projection within the anatomical images) that has been used in the orthopedic and neurosurgical settings. It is not known, however, whether this technology can be transferred into the urological domain for use with soft tissue. The purpose of this study was to assess the technical feasibility and safety of the OASSTS for percutaneous renal cryoablation in a porcine model.

Accepted for publication November 2011

Acknowledgement

Funding provided by Medtronic Inc.

Address correspondence to Dr. Kent T. Perry, Department of Urology, Northwestern University Feinberg School of Medicine, 675 North St. Clair Street, Suite 20-150, Chicago, IL 60611 USA

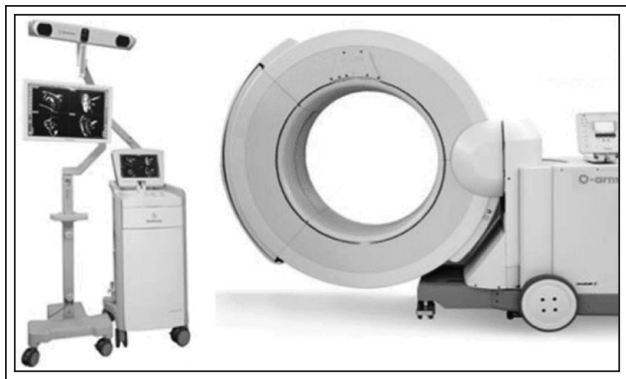


Figure 1. Surgical navigation with the O-Arm and StealthStation TREON System consists of the O-Arm on the right and the StealthStation TREON on the left.

Materials and methods

The study protocol was approved by our Institutional Animal Care and Use Committee. Six pigs (12 kidneys), weighing between 85.5 kg-99 kg (male and female) were utilized. The first pig (two kidneys) was used to develop and refine the steps of our protocol. As a result, we excluded this pig from our analyses.

Imaging and surgical navigation system

The OASSTS consists of two main components, the O-Arm, the imaging platform, and the StealthStation TREON, which creates and displays trajectory images for percutaneous surgery, Figure 1. The O-Arm is comprised of an “O”-shaped gantry which generates both 2D fluoroscopic (i.e. “scout”) and 3D images. The 3D images are an acquired volume data set that can be manipulated in any axis (in addition to the traditional transverse, coronal, and sagittal orthogonal planes). The images are obtained after having secured a bone-anchored dynamic reference frame (DRF) (a tracked object that holds small reflective spheres) to the pig’s iliac crest, Figure 2, see protocol procedure, below. The StealthStation TREON is a surgical navigation system that collects the imaging data from the O-Arm and creates a translation map between all points in the subject’s images and the corresponding points on the subject’s anatomy. After establishing this map, whenever the surgeon points to the patient’s anatomy using a tracked pointing device (enabled by its own optical reference frame with reflective spheres), the OASSTS uses the map to identify the corresponding point on the images. Because the OASSTS captures 3D data, navigation may be facilitated by trajectory images (displaying anatomy in the plane of the trajectory of the pointing device, while the pointing device itself is displayed as a projection within the

anatomical images). These images (displayed on a separate monitor) are altered instantaneously with the corresponding movements of the surgeon’s hand-held pointing device (“cryoprobe”, see below, Figure 2). The OASSTS does not provide real-time imaging like that of live fluoroscopy. Rather, imaging data is first captured by the O-Arm (which requires 13 seconds of breath-holding) and then (with ventilations resumed) transferred to the StealthStation TREON for processing. Once processed, the images may be navigated with the movements of the hand-held pointing device in a way that mimics real-time. Once a trajectory into the renal region of interest has been chosen, the subject’s breath is held again as the tracked pointing device is advanced into position.

Treatment modality

The Galil Renal Cryotherapy System (Galil Medical, MN, USA) was used as the treatment modality in this study. The hand-held pointing device (the “cryoprobe”) was crafted by attaching an optical reference frame to a 17-gauge cryoablation needle (IceRod, Galil Medical, MN, USA), see Figure 2.

Treatment regions

Because percutaneous focal renal ablation has traditionally been used for posterior or lateral tumors,⁴ we chose to direct our attention to these portions of the porcine kidney. For each kidney, the treated region was chosen randomly. Each kidney was treated only once for a total of 10 kidneys (five pigs) and 10 treated regions.



Figure 2. Upper-right: Our hand-held tracked pointing device (“cryoprobe”) crafted from a 17-gauge cryoablation needle (Galil Medical, MN, USA) with attached optical reference frame; Lower-left: Dynamic reference frame secured to animal’s iliac crest.

Protocol procedure

The animals were anesthetized and placed in the prone position on the operating table. The O-Arm was brought into position and AP and lateral 2D scout images were taken to center the ipsilateral kidney within the imaging field. The bone-anchored DRF was then inserted into the animal's iliac crest by making a 5 mm skin incision and using a lightweight surgical hammer. Ventilations were held for 13 seconds for an initial O-Arm 3D image capture. With ventilations resumed, the imaging data was then transferred to the StealthStation TREON System. Our modified hand-held 17-gauge cryoprobe was then registered and calibrated by the StealthStation. With ventilations held again, the cryoprobe was then manually inserted percutaneously into the renal region of interest using the trajectory images. Another O-Arm 3D image was captured to confirm the placement of the cryoprobe into the renal region of interest. A second cryoprobe was inserted and a third O-Arm 3D image was captured in the same manner to confirm placement of both cryoprobes. This was followed by a 30 minute cryotherapy treatment session (two cycles of 10 minutes of freezing and 5 minutes of active thawing). Finally, a fourth O-Arm 3D image was captured to display the cryotherapy iceball. This final image was captured at the end of the second freeze cycle. The cryoprobes were removed at the end of the final thaw cycle. All ventilation-holds were performed at end-expiration. These procedural steps were then repeated on the contralateral kidney. Insertion of the DRF into the iliac crest was required only once for each animal (i.e. only one DRF was inserted for both left and right kidneys). For none of the kidneys was repositioning of the animal necessary. Following the cryotherapy, the animals were euthanized and sent for necropsy. Necropsy consisted of both gross and histopathologic analyses.

Outcomes assessed

Several outcomes were measured:

Procedural times: We measured the time required to complete an entire treatment session (including all steps described in the protocol procedure, above) for each renal region of interest. We did not include the time required to insert the DRF as only one DRF was required for both left and right kidneys. The DRF insertion time was measured separately. The cryoablation treatment time was, by definition, 30 minutes.

Radiation exposure: The O-Arm produces a radiation exposure output report after each scan (whether 2D scout or 3D). For 2D scout images, the dose-area product

(DAP, $\text{mGy}\cdot\text{cm}^2$) was recorded. For 3D images, the dose-length product (DLP, $\text{mGy}\cdot\text{cm}$) was recorded. Cumulative exposure for each treatment session is also reported. Because we are ultimately interested in radiation exposure incurred by patients, corresponding conversion factors were used to calculate the effective dose adjusted for humans (EDH, mSv).^{5,6} We also measured exposure to the OASSTS technician with thermoluminescent dosimeter chips worn outside of their lead aprons. A technician is required to be in the same room during scanning in order to control the OASSTS from the O-Arm console.

Complications: Any injury to surrounding organs, such as bowel, spleen or liver, was assessed at the time of gross pathological analysis during necropsy. Injury to the ipsilateral kidney was also identified.

Concordance: We compared the anticipated iceball location (as determined by the projections of the cryoprobes on the trajectory images before freezing was initiated) to the location of the cryoablated lesion as determined on necropsy.

Results

Procedure times

Over the course of the study, five pigs were utilized and thus five DRF pins were placed. The mean time to place the DRF was 3.85 minutes (range 2.6-5.3 minutes). The mean procedure time (excluding the duration of the cryotherapy treatment component, which by definition was 30 minutes) was 24.0 minutes (range 16.7-31.5 minutes). The mean total procedure time was, therefore, 27.85 minutes (procedure time + DRF time). The mean total treatment time was 57.85 minutes (procedure time + DRF time + cryotherapy time).

Radiation exposure

The mean total (2D scout and 3D) radiation exposure to the animals (for the treatment of each kidney) was 23.69 mSv (0.14 mSv and 23.55 mSv for 2D scout and 3D images, respectively; range 12.83 mSv-41.31 mSv). The mean total radiation exposure to the technician operating the O-Arm was less than 1 mrem, indicating that his exposure was equivalent to background radiation levels only.

Complications

One kidney was associated with a cryoablation-related injury to the adjacent lumbar muscle and another involved the renal pelvis. In an additional case, inadequate cryoprobe positioning was identified after a 3D image capture, but before cryotherapy was

initiated. The cryoprobe was withdrawn slightly (but not removed from the kidney) and an additional 3D image capture was performed to reconfirm appropriate positioning.

Concordance

For each renal region of interest, two cryoprobes were inserted. Thus, for all 10 kidneys in this study, 20 cryoprobe insertions were performed. Among them, in only one attempt/insertion was cryoprobe position found to be inadequate (as determined on one of the O-Arm 3D image captures performed prior to the cryotherapy cycle, as described above) and repositioning was thus required. In all 10 renal regions treated, the location of the anticipated iceball on trajectory imaging (as assessed by the placement of the cryoprobes on the trajectory images before freezing) corresponded to the location of the iceball on the O-Arm during the freeze cycle and to the cryolesion found on necropsy. The mean cryoablation lesion diameter and depth (from the level of the renal capsule) was 40.1 mm and 17.8 mm, respectively, Table 1. Histopathological analysis of the cryolesions confirmed coagulative necrosis. See Figure 3 for a representative specimen and corresponding trajectory images.

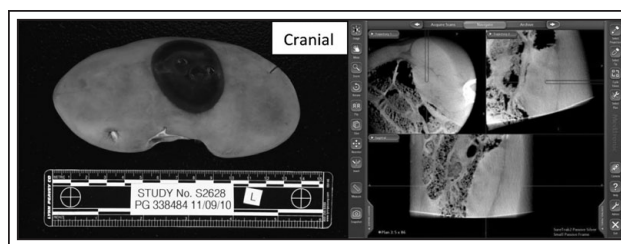


Figure 3. Left: Representative specimen showing cryoablation lesion on necropsy in the left kidney, mid-pole, postero-lateral surface (the cranial aspect is marked). Right: The corresponding trajectory images (the trajectory of the cryoprobe appears blue as it is advanced into the kidney). Note that two trajectory images are shown (top) and a standard sagittal image is displayed (bottom) for comparison.

Discussion

In this pilot study, we demonstrated the use of trajectory image-based percutaneous renal cryoablation using the OASSTS in a porcine model. Trajectory image-based surgery with the OASSTS has already been described in the orthopedic and neurosurgical literature,⁷ but to our knowledge, this is the first description of its

TABLE 1. Concordance: cryoablation lesions and complications

Kidney ^a	Renal region treated on trajectory images ^b	Location of cryoablation lesion on necropsy ^b	Size of cryoablation lesion on necropsy (mm) ^c		Complications
			Diameter	Depth (within capsule)	
3	UP-apical	UP-apical	44	29.5	None
4	MP-posterior surface	MP-posterior surface	43.2	15.2	None
5	MP to LP-L	MP to LP-L	42.83	21.2	None
6	LP-L	LP-L	50	14.9	None
7	MP-L	MP-L	35.2	19.1	Lumbar muscle
8	LP-M	LP-M	39.3	18.5	None
9	LP to MP-L	LP to MP-L	39.2	19.9	None
10	UP-M	UP-M	31.3	12.4	None
11	LP-L	LP-L	44.6	13.0	None
12	UP-L	UP-L	31.7	14.4	Renal pelvis

^athe first pig (kidneys 1 and 2) were used to develop and refine out protocol and were not included in the analyses

^bUP = upper pole; MP = midpole; LP = lower pole; M = medial; L = lateral

^cnote that two cryoprobes were used for each treated renal region

use for a soft tissue indication in a urological setting. We attempted to assess its technical feasibility and safety. As a secondary outcome, we also assessed its accuracy by comparing the location of the cryoablation iceball (based on the location of the cryoprobes on the trajectory-based images) to the location of the cryoablated lesion on necropsy. We found that using the OASSTS required a short treatment time, was technically feasible and was safe, but that more detailed accuracy outcomes are needed before this technology can be considered for use in humans.

At the time this study was performed, no proprietary device which allowed for a trackable cryoablation needle existed. As a result, we crafted one using needles that were already familiar to urologists by attaching an optical reference frame to them. After optically calibrating and registering these "cryoprobes" with the OASSTS' DRF, we were able to use them as pointing devices which defined a trajectory through the pig's anatomy depending on the angle they were held by the surgeon. While the DRF required a small incision and insertion into the iliac crest, we do not believe that this would be a limitation in humans as similar bone anchoring is already used in the orthopedic and neurosurgical settings. The total procedure times (excluding the cryotherapy time which is always known) were short (mean 27.9 minutes), and included cryoprobe calibration and registration, percutaneous cryoprobe placement into the renal region of interest, and all of the 3D image captures that were required to confirm cryoprobe placement. Including the cryotherapy cycles, the mean total treatment time was 57.9 minutes. This is less than that reported in a study comparing cryoablation approaches which described significantly longer treatment times of 147 and 252 minutes, for CT-guided percutaneous and laparoscopic cryoablation, respectively⁸.

The OASSTS is currently not modified for specific use with soft tissue, such as the kidney, and the software used in this study was the "bone window" software already in use. This software, however, still provided us with adequate soft tissue imaging and allowed the surgeons to easily identify surrounding organs including bowel, liver and spleen. There were no occurrences of bowel moving into the iceball region after the initial trajectory images were acquired. We also did not have any instances of misrecognition of the OASSTS. There were also no inadvertent movements of the animals during the procedures. While the chest may also be easily imaged, the more inferior position of the kidneys in pigs as compared to humans did not present us with any risk of injuring the pleura. Because the other major soft tissue organs of the abdomen are

imaged, avoidance of them can be accomplished as the cryoprobe is advanced into the renal region of interest for treatment. Furthermore, it also imaged the cryoprobes without difficulty and subsequent scanning with the O-Arm (before cryotherapy was initiated) provided the surgeon with feedback to reposition the cryoprobe if the initial position of the needle was not satisfactory.

In one kidney, we also observed a cryolesion injury to the adjacent lumbar muscle. In this study, we used the IceRod cryoneedle which produces an iceball with an exaggerated ellipsoid shape. We believe that switching to an IceSphere or IceSeed configuration may have prevented this injury by restricting the size of the iceball. The clinical significance of this finding is unclear.

We also measured the effective dose of radiation to which the animals were exposed and found it to be modest (as it included four 3D scans). The mean effective dose for an entire treatment session was under 24 mSv. A recent study describing the radiation dose associated with CT-guided percutaneous renal mass ablation reported a mean effective radiation dose of 53 mSv (more than double what is reported in this study) with 69% of the radiation (36 mSv) occurring during probe positioning.⁹ Another study reported a mean radiation exposure of 2374 mGy·cm (approximately equivalent to 35.6 mSv) associated with CT-guided percutaneous renal mass cryoablation.¹⁰ In comparison, a large retrospective study¹¹ of CT doses reported that a patient can receive as much as 10-20 (mean 15) mSv for a single abdominal-pelvic CT. As well, some studies of CT-guided percutaneous renal cryoablation describe the use of 4-5 abdominal CTs per treatment session.¹² A similar navigation device, the CT-Nav (Koelis, La Tronche, France) has also been described¹³ for use in kidneys, however, the authors did not report effective dose, but did report radiation exposure time, instead. The radiation exposure to the O-Arm operator (the only personnel in the operating room during each O-Arm image capture) was also negligible.

This study has shown that the major strengths of this technology for renal indications are the very short treatment times and minimal amounts of radiation exposure. Use of the OASSTS was technically feasible and intuitive in its execution. While it is capable at tracking the moving cryoprobe, the major limitation of the device is its inability to track a moving target such as the kidney. As a result, accuracy is dependent on breath-holding such that the kidney lies in the same position during placement of the cryoprobe as it was during the initial acquisition of the 3D images upon

which the trajectory images are constructed. This problem is partially overcome as additional imaging can easily be performed after cryoprobe placement to confirm its correct position.

A limitation of our study was the lack of a renal target that was visualized by the O-Arm. As a measure of accuracy we instead relied upon the concordance between trajectory-based imaging and findings on necropsy. With this limitation in mind, our data suggests that OASSTS guidance correlates to both the intra-operative OASSTS imaging and to cryolesion location. Finally, the capital expense of OASSTS is approximately \$600,000. When used in humans, the extent to which this may be offset with, for example, shorter hospital admissions, is not known.

In summary, this pilot study demonstrated that trajectory image-based percutaneous cryoablation using the OASSTS was technically feasible in the porcine model. It may also provide accurate cryoprobe placement into renal regions of interest. While this technology has promise for soft tissue surgical navigation, additional studies to clarify and better define its accuracy are required before use in humans. □

10. Schroeder G, Agarwal G, Smith J et al. Determination of patient radiation dose in radiofrequency and cryoablation of small renal masses. Presented at the American Urological Association, Washington, DC, May, 18, 2011
11. Smith-Bindman R, Lipson J, Marcus R et al. Radiation dose associated with common computed tomography examinations and the associated lifetime attributable risk of cancer. *Arch Intern Med* 2009;169(22):2078-2086.
12. Mues AC, Landman J. Image-guided percutaneous ablation of renal tumors: outcomes, technique, and application in urologic practice. *Curr Urol Rep* 2010;11(1):8-14.
13. Haber GP, Crouzet S, Remer EM et al. Stereotactic percutaneous cryoablation for renal tumors: initial clinical experience. *J Urol* 2010;183(3):884-888.

References

1. Janzen N, Zisman A, Pantuck AJ, Perry K, Schulam P, Beldegrun AS. Minimally invasive ablative approaches in the treatment of renal cell carcinoma. *Curr Urol Rep* 2002;3(1):13-20.
2. Lotan Y, Cadeddu JA. A cost comparison of nephron-sparing surgical techniques for renal tumour. *BJU Int* 2005;95(7):1039-1042.
3. Hui GC, Tuncali K, Tatli S, Morrison PR, Silverman SG. Comparison of percutaneous and surgical approaches to renal tumor ablation: metaanalysis of effectiveness and complication rates. *J Vasc Interv Radiol* 2008;19(9):1311-1320.
4. Schmit GD, Atwell TD, Leibovich BC et al. Percutaneous cryoablation of anterior renal masses: technique, efficacy, and safety. *AJR Am J Roentgenol* 2010;195(6):1418-1422.
5. Huda W, Gkanatsios NA. Effective dose and energy imparted in diagnostic radiology. *Med Phys* 1997;24(8):1311-1316.
6. McCollough C. (ed.). The Measurement, Reporting, and Management of Radiation Dose in CT. College Park, MD: American Association of Physicists in Medicine, 2008.
7. Nottmeier EW, Seemer W, Young PM. Placement of thoracolumbar pedicle screws using three-dimensional image guidance: experience in a large patient cohort. *J Neurosurg Spine* 2009;10(1):33-39.
8. Finley DS, Beck S, Box G et al. Percutaneous and laparoscopic cryoablation of small renal masses. *J Urol* 2008;180(2):492-498.
9. Hoch S, Durack J, Sorensen M, Gould R, Stoller M. Radiation dose associated with CT-guided percutaneous renal mass ablation and imaging follow-up. Presented at the American Urological Association, Washington, DC, May 18, 2011.